Applied Microscopy
Korean Society of Microscopy

pISSN 2287-5123 · eISSN 2287-4445
http://dx.doi.org/10.9729/AM.2013.43.1.9

Biological Applications of Helium Ion Microscopy

Ki Woo Kim*

School of Ecology and Environmental System, Kyungpook National University, Sangju 742-711, Korea

*Correspondence to:
Kim KW,
Tel: +82-54-530-1246
Fax: +82-54-530-1248
E-mail: kiwoo@knu.ac.kr

Received February 13, 2013
Revised March 4, 2013
Accepted March 11, 2013

The helium ion microscope (HIM) has recently emerged as a novel tool for imaging and analysis. Based on a bright ion source and small probe, the HIM offers advantages over the conventional field emission scanning electron microscope. The key features of the HIM include (1) high resolution (ca. 0.25 nm), (2) great surface sensitivity, (3) great contrast, (4) large depth-of-field, (5) efficient charge control, (6) reduced specimen damage, and (7) nanomachining capability. Due to the charge neutralization by flood electron beam, there is no need for conductive metal coating for the observation of insulating biological specimens by HIM. There is growing evidence that the HIM has substantial potential for high-resolution imaging of uncoated insulating biological specimens at the nanoscale.

Key Words: Charging, Contrast, Helium, Probe, Resolution

INTRODUCTION

The need for high-resolution images of nanostructures has pushed the boundaries of charged particle microscopy (Scipioni et al., 2007). The probe size of the field emission scanning electron microscope (FESEM) is on the order of 1 nm; however, there are intrinsic limitations to the high-resolution imaging due to lens aberrations, diffraction effects, and the nature of specimen-electron beam interactions (Bell, 2009). Conductive metal coatings for FESEM obscure fine morphological details, inflate diameter measurements, and may introduce artifacts (Vanden Berg-Foels et al., 2012). The helium ion microscope (HIM) is a recently introduced microscope that uses a scanning helium (He) ion beam for surface imaging and analysis. It dates back to 1951, when a field ion microscope, the underlying technology of the HIM, was first reported (Economou et al., 2012). The HIM has a number of advantages over the conventional FESEM for imaging and analyzing biological specimens, including (1) higher resolution (ca. 0.25 nm), (2) greater surface sensitivity, (3) greater contrast, (4) larger depth-of-field, (5) efficient charge control, (6) reduced specimen damage, and (7) nanomachining capability (Bell, 2009; Vanden Berg-Foels et al., 2012). There is growing evidence that the HIM has substantial potential for high-resolution imaging of uncoated insulating biological specimens at the nanoscale (Bazou et al., 2011; Alkemade et al., 2012; Boden et al., 2012; Kim, 2012).

Fig. 1. Helium ion microscope. It consists of a main body, a pattern generator (for nanofabrication), and a gas injection system (reproduced from the Environmental Molecular Sciences Laboratory at the Pacific Northwest National Laboratory, US).

BASICS OF HIM

The external appearance of the HIM is overall similar to that of FESEM (Fig. 1). The ALIS Corporation has developed the core technology of the HIM such as the He ion source. Thereafter, the microscope (now dubbed ORION PLUS) was first commercialized and has been currently produced by Carl Zeiss SMT (Oberkochen, Germany) (Bell, 2009; Economou et al., 2012). The HIM system consists of a main body, a pattern generator for nanofabrication, and a gas injection system. The key features of the HIM include a high brightness ion source (Fig. 2). The design principle is based on the field ion microscope operating in an ultrahigh vacuum environment with a cryogenically cooled sharp tungsten tip having three

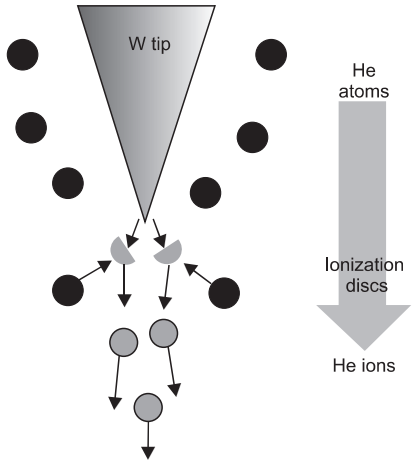

Fig. 2. Schematic diagram of the helium ion source. Helium atoms in the vicinity of the cooled and sharp tungsten (W) tip are ionized by the ionization discs and accelerated under an electric field.

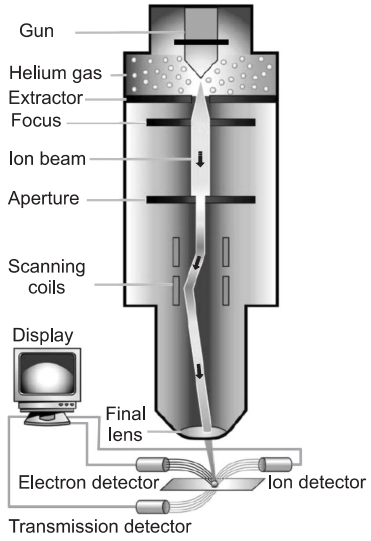

Fig. 3. Schematic diagram of the helium ion microscope. It has an ion gun, a column, and a display unit (modified from Morgan et al. *Microsc. Today* **14(4)**, 24-31, 2006).

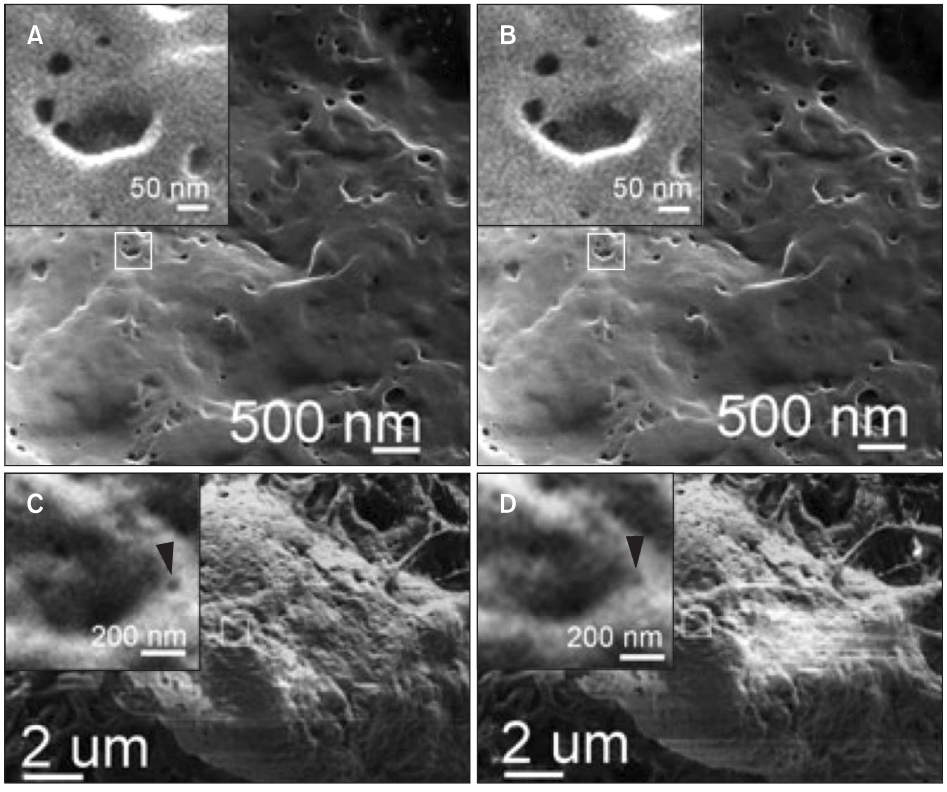

Fig. 4. Images of uncoated human colon cancer cells. (A, B) Helium ion micrographs after the first and second scan, respectively. Slight damages are noted in magnified areas (inlets). (C, D) Scanning electron micrographs after the first and second scan, respectively. Notable damages are shown in inlets (reproduced from Bazou et al. *J. Microsc.* **242**, 290-294, 2011, with permission from the publisher).

atoms (trimer) at the apex, to which small amounts of He gases are introduced (Bell, 2009). Applying a high voltage to the tip emits ionization discs that ionize nearby He gas atoms by the process of electron tunneling; the resulting He ions are immediately accelerated away from the tip (Fig. 3) (Morgan et al., 2006). The HIM has detectors for secondary electrons, backscattered He ions, and transmitted He ions.

Because the virtual source size is very small and each ionization region is smaller than the atom spacing, the He ion beams have a remarkable brightness of ~1.4×10^9 A/cm^2/sr, which is ~30 times better than the Schottky field emission gun (Morgan et al., 2006; Ward et al., 2006; Bell, 2009; Vanden

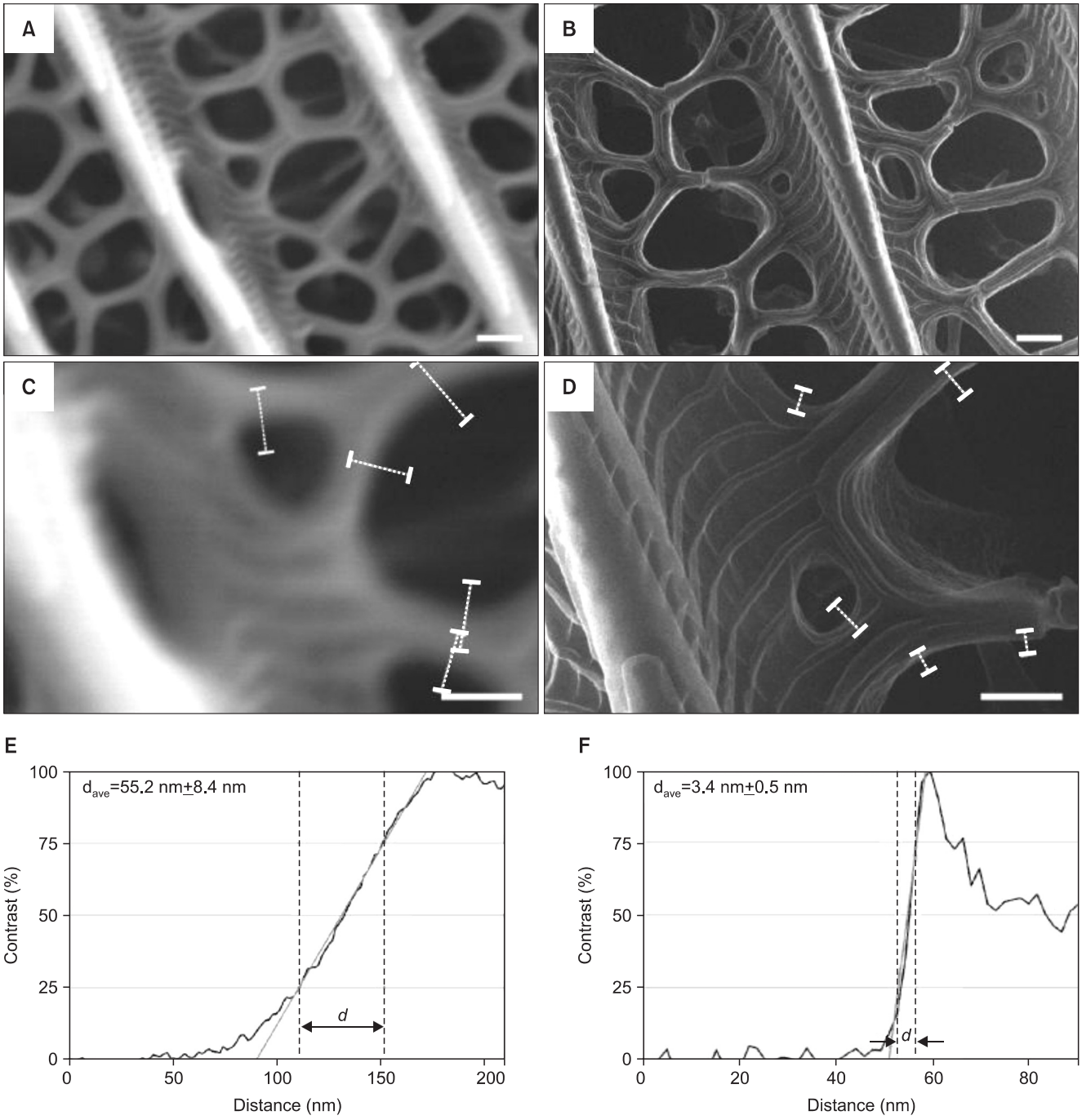

Fig. 5. Images of uncoated butterfly scales. (A, C) Helium ion micrographs. (B, D) Variable-pressure scanning electron micrographs. Edge lines in (C) and (D) are for the calculation of image sharpness. Bars in (A) and (B)=500 nm. Bars in (C) and (D)=300 nm. (E) Contrast measurement in the line profiles of (C). (F) Contrast measurement in the line profiles of (D) (reproduced from Boden et al. *Scanning* **34**, 107-120, 2012, with permission from the publisher).

Berg-Foels et al., 2012). The He ion beams can be brought to focus with a probe size of less than 0.25 nm in diameter (Postek & Vladár, 2008). The energy spread of the HIM beams is on the order of 1.0 eV (Bell, 2009). Due to the small wavelength and convergence angle on the specimen, the He ion beams have extremely large depth-of-field in the secondary electron images while still retaining surface detail (Bell, 2009). Since the interaction volume of the HIM ion beams is smaller than that of FESEM, secondary electrons are emanated at the point of initial interaction with the specimen, leading to enhanced surface sensitivity (Postek & Vladár, 2008). Because the energy of He ions is much higher than that of electrons in SEM, the He ions penetrate much more deeply into the specimen with far less lateral straggle (Morgan et al., 2006). The secondary electron image by HIM at 20 kV more closely resembles the secondary electron image by SEM at 0.5 kV, due to the similar escape depth of secondary electrons (Bell, 2009). For each incoming He ion, 2 to 8 secondary electrons are generated; however, for each incoming electron, one secondary electron is made available under typical SEM conditions (Morgan et al., 2006). Such a nature of HIM allows for high contrast imaging with low probe currents (Postek & Vladár, 2008). In addition, a beam consisting of noble gas ions is preferred to minimize any chemical, electrical, or optical alteration of the specimen, leading to the reduced sputtering (Morgan et al., 2006). The He ion beam has orders of magnitude smaller etching effect than the currently available gallium ion beam (Postek & Vladár, 2008).

SPECIMEN PREPARATION FOR HIM

The merit of the HIM is to observe insulating biological specimens without conductive metal coating. Because of the ease of neutralizing the specimen charge using a flood electron beam, surface charging effects are minimal and therefore cell surfaces can be imaged without the need for a conductive metallic coating (Chen et al., 2011). Prior to observation by HIM, specimens should be processed, dried by either critical point drying or freeze-drying, and mounted on stubs. The imaging of specimens coated with gold is relatively straightforward as the specimens are sufficiently grounded to allow any charge build-up to dissipate (Bazou et al., 2011).

BIOLOGICAL APPLICATIONS

HIM versus FESEM

Human colon cancer cells were chemically fixed and freeze-dried (Bazou et al., 2011). The HIM showed surface details of uncoated cells (Fig. 4A and B). No detectable specimen damage was observed on the cell surface even after the scans. In contrast, the damage by the electron beam was noted on the cell surface (Fig. 4C and D). Some of the pores on the cell surface disappeared after consecutive scans. This work demonstrates that the HIM can reveal much more details including surface pores with undetectable specimen damage.

HIM versus VP-SEM

Butterfly scales were deposited onto carbon tabs attached to SEM metal stubs (Boden et al., 2012). Without metal coating, they were left overnight before loading into the HIM. The limitations of spatial resolution and depth-of-field were apparent in the variable pressure SEM (Fig. 5A and C). Meanwhile, the entire specimen appears in focus and surface details were discerned (Figs. 5B and D). The measurements of the contrast change (line profile) across edges revealed a factor of ~16 differences between the two microscopes, with the edge sharpness of the variable pressure-SEM image measured as 55.2±8.4 nm (Fig. 5E), compared with 3.4 nm±0.5 nm for the HIM (Fig. 5F). Further studies will be done to image at higher magnifications to resolve unknown differences between species.

Depth-of-field

Collagen fibers from the knee joint of a mouse were metal coated and observed by HIM (Bosco, 2011). It was feasible to acquire images showing structural details of the banding (Fig. 6A) (Scipioni, 2009). Uncoated collagen fibers were also imaged by HIM (Vanden Berg-Foels et al., 2012). The entire

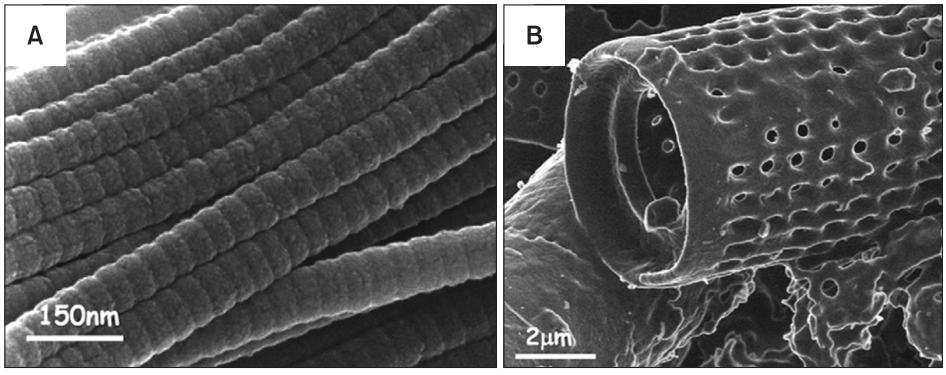

Fig. 6. Helium ion micrographs. (A) Collagen fibers from the knee joint of a mouse. (B) Diatoms. The depth-of-field of the helium ion microscope is greater than that of scanning electron microscope (reproduced from Bosco. *Trends Analyt. Chem.* **30**, 1189-1211, 2011, with permission from the publisher).

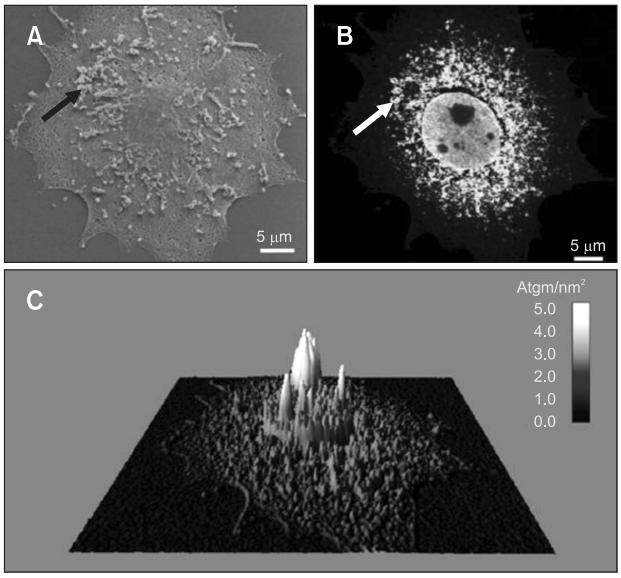

Fig. 7. Imaging of human fetal liver cells by using fast and slow focused helium ions. (A) Secondary electron image of the helium ion microscope at 45 kV. Arrows in (A) and (B) indicate a surface feature, respectively. (B) Transmitted helium ion image of the same cell at 1.2 MeV. (C) Mass image showing a three-dimensional plot of the mass distribution (in units Atg/nm^2; 1 Atg=10^{-18} g) at 1.2 MeV (reproduced from Chen et al. *Biophys. J.* **101**, 1788-1793, 2011, with permission from the publisher).

areas of diatoms were in focus (Fig. 6B). These results indicate that the depth-of-field of the HIM was ~50~100×higher than SEM.

Whole-cell Imaging

Surface details of critical point dried-human fetal liver cells were imaged by HIM operating at 45 kV (Chen et al., 2011). For subcellular imaging of the specimens, the 1.2 mega V (MeV) He ion beams were produced by an ion accelerator. Secondary electron images from the kV He ions revealed the surface details of the specimen (Fig. 7A). Transmitted He ions were collected to show subcellular features (Fig. 7B) and mass distribution in the cell (Fig. 7C) by measuring the energy loss as the He ions pass through the cell. This work suggests microscopy using the He ions could enhance both surface and subcellular imaging. The prototype MeV HIM is in progress to improve the spatial resolution by increasing the He ion source brightness.

CONCLUSIONS

It is obvious to state that the HIM will make significant contributions to the most challenging imaging and nanobiotechnology applications (Economou et al., 2012). Due to the high-resolution and large depth-of-field imaging at the nanometer scale, the HIM enables the rapid and detailed morphological analysis of a variety of insulating and beam-sensitive biological specimens with reduced labor and preparation. Combined with spectroscopy and nanofabrication capabilities, the HIM would be a novel choice for imaging and analysis in the future biologist's toolkit.

REFERENCES

Alkemade P F A, Koster E M, Van Veldhoven E, and Maas D J (2012) Imaging and nanofabrication with the helium ion microscope of the Van Leeuwenhoek Laboratory in Delft. *Scanning* **34**, 90-100.

Bazou D, Behan G, Reid C, Boland J J, and Zhang H Z (2011) Imaging of human colon cancer cells using He-Ion scanning microscopy. *J. Microsc.* **242**, 290-294.

Bell D C (2009) Contrast mechanisms and image formation in helium ion microscopy. *Microsc. Microanal.* **15**, 147-153.

Boden S A, Asadollahbaik A, Rutt H N, and Bagnall D M (2012) Helium ion microscopy of Lepidoptera scales. *Scanning* **34**, 107-120.

Bosco G L (2011) Imaging in the modern age. *Trends Analyt. Chem.* **30**, 1189-1211.

Chen X, Udalagama C N B, Chen C-B, Bettiol A A , Pickard D S, Venkatesan T, and Watt F (2011) Whole-cell imaging at nanometer resolutions using fast and slow focused helium ions. *Biophys. J.* **101**, 1788-1793.

Economou N P, Notte J A, and Thompson W B (2012) The history and development of the helium ion microscope. *Scanning* **34**, 83-89.

Kim K W (2012) Helium ion microscopy of uncoated pine leaves. *Appl. Microsc.* **42**, 147-150.

Morgan J, Notte J, Hill R, and Ward B (2006) An introduction to the helium ion microscope. *Microsc. Today* **14(4)**, 24-31.

Postek M T and Vladár A E (2008) Helium ion microscopy and its application to nanotechnology and nanometrology. *Scanning* **30**, 457-462.

Scipioni L (2009) Principles and applications of helium ion microscopy. Available from: http://www.microscopy-analysis.com/features/principles-and-applications-helium-ion-microscopy/.

Scipioni L, Stern L, and Notte J (2007) Applications of the helium ion microscope. *Microsc. Today* **15(6)**, 12-15.

Vanden Berg-Foels W S, Scipioni L, Huynh C, and Wen X (2012) Helium ion microscopy for high-resolution visualization of the articular cartilage collagen network. *J. Microsc.* **246**, 168-176.

Ward B W, Notte J A, and Economou N P (2006) Helium ion microscope: a new tool for nanoscale microscopy and metrology. *J. Vac. Sci. Technol. B* **24**, 2871-2874.